Available online at www.easd.procedia.org
EASD Procedia EURODYN (2026) 1726-1739

EASD Procedia

EURODYN 2026
XIII International Conference on Structural Dynamics
M. Beer, C. Papadimitriou, H. Jensen, J. Chen, M. Broggi, J. Behrensdorf (eds.)
Hannover, Germany, 27.09.–01.10 2026

STRUCTURAL HEALTH MONITORING OF AN ARCH BRIDGE WITH ARTIFICIAL INTELLIGENCE-BASED ANOMALY DETECTION IMPLEMENTED IN A REAL-TIME MONITORING SYSTEM ARCHITECTURE

Diego Zamora-Sánchez[1], Alberto Armijo[1], José Carlos Jiménez-Fernández[1], Jesús Lucena[1], Mikel Ezquerro[1]

[1] TECNALIA, Basque Research and Technology Alliance (BRTA)
e-mail: diego.zamora@tecnalia.com, alberto.armijo@tecnalia.com, josecarlos.jimenez@tecnalia.com

Keywords: Arch bridge, Real-time monitoring architecture, Artificial neural network, Unsupervised learning, Finite element modeling.

Abstract. *The Etxebarri arch bridge is a reinforced and prestressed concrete bridge approximately 88 m long, with an arch spanning more than 56 m and extended at each end by a 15.50 m span to cross the Nervión River between the municipalities of Etxebarri and Bilbao (Spain).*

During the second half of 2025, a monitoring system was installed on this bridge to continuously monitor its structure and improve safety during the railway renovation works that began that year. These works are carried out at night, while during the day the bridge returns to operation.

This paper explains the real-time monitoring system implemented, which uses the 4G network and Message Queuing Telemetry Transport (MQTT) communication to send high-sampling data. Accelerations and inclinations are measured on the bridge deck using both high-end wired sensors and, as a supplement, IoT devices. Then, an initial warning system based on the vertical deck acceleration limits of the Eurocode has been established.

For this research, the obtained eigenfrequencies are first contrasted with the results given by finite element models of the bridge, and these are compared with information from the opening load test in 2003. Finally, an anomaly detection method based on an unsupervised neural network has been functionally included in the monitoring system. This approach considers the full acceleration time series, treating them as response signatures in the time domain, yielding promising results. This technique, together with the modular real-time monitoring system implemented, constitutes a solution that could be easily adapted to other sensors and structures.

ISSN:2311-9020 © 2026 The Authors. Published by EASD Procedia.
Peer-review under responsibility of the Organizing Committee of EURODYN 2026.
doi: 10.47964/1326.10781.485

1 INTRODUCTION

The Etxebarri arch bridge (Bilbao), designed by Leonardo Fernández Troyano and Javier Manterola Armisén, is a large prestressed and reinforced concrete arch with a span of 56.50 meters, extended at each end by a span of 15.50 meters, to cross the Nervión River on the border between the municipalities of Etxebarri and Bilbao. The bridge crosses the river at an angle of 63º, which has been achieved by staggering the two rings of the arch longitudinally, resulting in staggered foundations and oblique abutments. The two rings of the arch coincide with the girders located under each of the tracks and are the same width, 1.60 meters, except at the lower edge of the arch, where they widen slightly. The arch is clamped at both ends and the deck is integrated into it and simply supported on the bridge abutments.

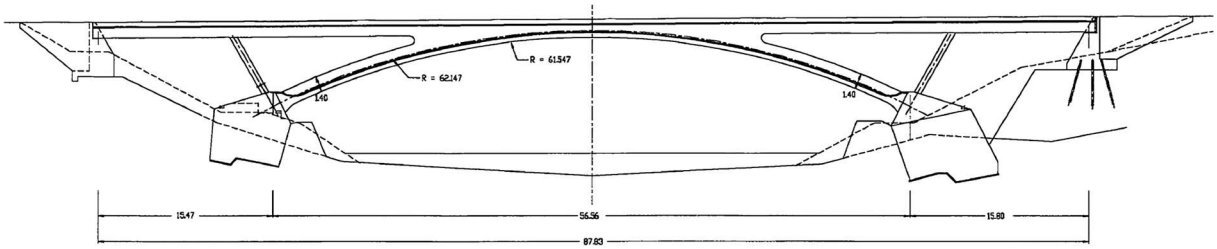


Figure 1: Elevation of the Etxebarri arch bridge built in 2003 (dimensions in meters according to the project drawings by engineering firm Fulcrum and designers L. Fernández Troyano and J. Manterola Armisén).

This structure needs to be monitored to improve ongoing maintenance and increase safety while the subway track on the bridge is being renovated. An instrumentation option was selected that allows for quick and structurally non-invasive installation, without interfering with the work in progress, as the track renovation work was already underway when TECNALIA was asked to monitor the structure. This article covers approximately the first six months of monitoring, which began at the end of June 2025 and is still ongoing at the time of writing.



Figure 2: Photograph of the Etxebarri arch bridge (Source: TECNALIA).

2 METHODOLOGY

Regarding the various methods of structural health monitoring (SHM), vibration-based monitoring (VBM) of civil infrastructures [1] is being utilized extensively on bridges [2]. One of its basic premises is that, under linear conditions, vibration characteristics depend solely on the stiffness matrix and mass matrix of the structure within the approaches of operational modal analysis (OMA), even though we must deal with variations caused by environmental

and operational factors [3]. Also, accelerometers, due to their better dynamic response, are the most commonly used sensors to obtain natural frequencies and mode shapes, although the oscillations associated with them are also present in other physical variables. However, other measurement quantities, such as strains or inclinations, are usually studied in the time domain, although there are more innovative applications in the frequency domain, such as the use of strain mode shapes [4].

In this work, in addition to a practical case study on bridge monitoring with a high-capacity data transmission system architecture, we will focus on considering only two accelerometers using artificial intelligence (AI) techniques. This is an advantage over approaches that take mode shapes into account, which require a higher density of points (sensors) to characterize them. Here, we consider that the measurement of accelerations, treated as a point-to-point time series to feed a real-time deployable convolutional neural network (CNN), contains both a valid reference for the vibratory characteristics (implicit in the signal) and for the operational variations in intensity. In this way, we will combine the global and local information of the structure by considering a single type of physical magnitude. In general, the combined use of local variables, such as inclinations or strains, with global variables, such as natural frequencies, is more reliable when AI techniques are applied [5].

The scientific literature contains works similar to the one presented here. For example, [6], where an offline CNN is applied to railway bridge acceleration records acceleration that have been previously transformed to mimic an image recognition technique, where this type of AI algorithm is more commonly used. Also noteworthy is [7], where a CNN is applied directly to raw data from decentralized wireless sensors. In this second case, the measurements come solely from laboratory experiments, and it is also debatable whether wireless sensors that can be deployed for permanent monitoring can measure environmental vibrations with sufficient accuracy and communication capability.

2.1 Description of the sensors and monitoring system architecture

Specifically, two wired high-sensitivity triaxial force-balance accelerometers (GeoSIG AC-73 model) have been installed near the center and at one quarter of the bridge span. A dual-axis clinometer with a liquid-filled electrolytic transducer from Jewell Instruments is also used. These measurements are complemented by BeanScape's microelectromechanical system (MEMS) type wireless IoT accelerometers and clinometers. All this data is transmitted to a real-time monitoring system to set alert thresholds, but only the force-balance accelerometers are used for AI processes (accuracy and stable data communication with a high sampling rate are required). In this bridge monitoring application, data from the two wired accelerometers and the inclinometer are transmitted in real time at a rate of 200 samples per second.

A HBK QuantumX universal acquisition module, a PC, a router, and a 4G antenna are housed in a control cabinet installed on an extension of the existing platform at one end of the bridge. We have grounded the shielding of the cable coming from the wired sensors on the control cabinet side to eliminate possible interference from the catenary. A wireless antenna connected to the control cabinet has also been installed on the bridge railing in the center of the span to enable the complementary IoT sensor network. In this way, centralized signals can be transmitted with a large number of samples per second via the 4G network and the MQTT (Message Queuing Telemetry Transport) protocol. The server performs most of the processing with this system architecture, except for some pre-processing filters that are performed on the control cabinet PC. This allows us to easily adapt to future changes in the sensors, mainly by making changes to the middleware (the layer linking sensors to the cloud). For added security, measurements are also stored locally on SSD hard drives, and the control

cabinet is equipped with an uninterruptible power supply (UPS) unit. Finally, the measurement system is configured to automatically restart and perform the task in the event of a total power and battery failure once power is restored.

The main platform for continuous monitoring is a real-time monitoring system architecture that is modular and adaptable. It was designed in previous work by the main authors [8] and has now been modified for this case study and a new AI implementation. This system can integrate many types of sensors, networks, and communication protocols with fluid changes in the middleware. The architecture allows for the implementation of AI algorithms, in this case a convolutional neural network for acceleration signature, and the subsequent storage of data in a dynamic time-stamped database. In addition, it is capable of providing data contextualization in Digital Twin environments, allowing for the use of various graphic formats, but this capability will be implemented for this bridge within future work. The system architecture is detailed in the figure below. For data input and processing adapted to the current instrumentation, the local network (A) uses middleware (Node-RED) hosted on TECNALIA's infrastructure. The data is then stored in a time series database (InfluxDB). The cloud network (B) consists of infrastructure leased from Azure for machine learning, batch processing, and scalable storage. A digital twin application (C) that enables various forms of graphical contextualization completes the system design.

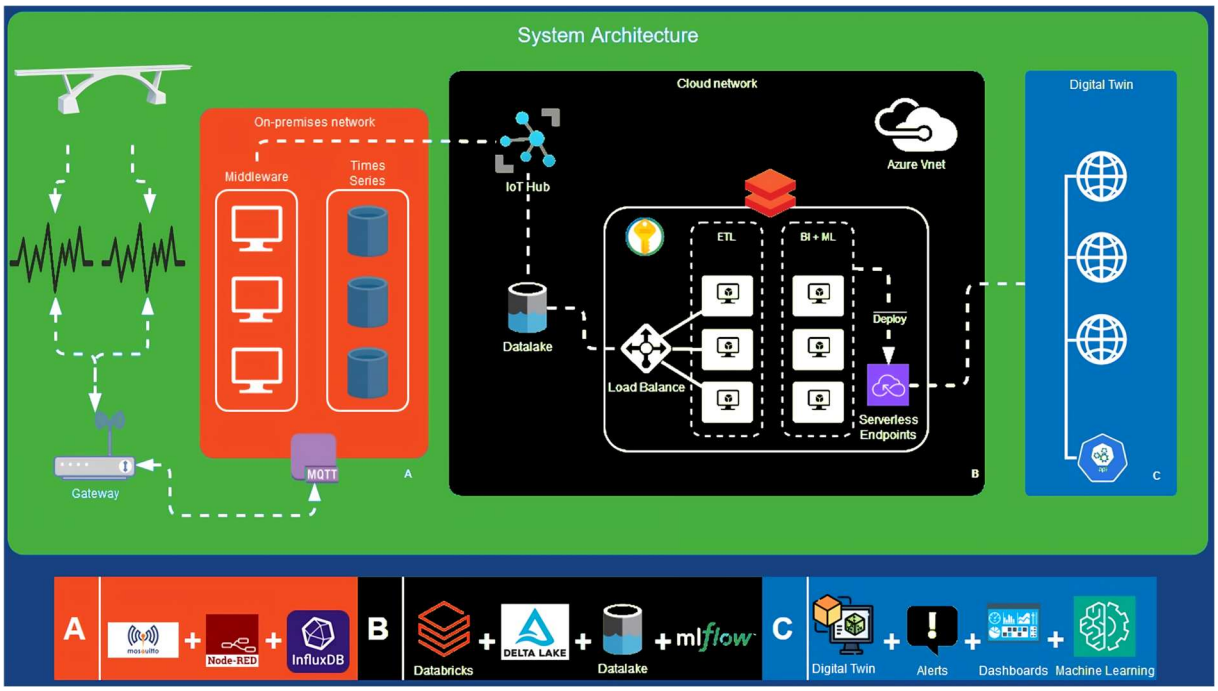


Figure 3: Hybrid on-premises and cloud network architecture customized for this bridge monitoring case.

2.2 Initial measurements and finite element models

When the actions to be considered, their combinations, and the characteristics of the materials are prescribed by standards, finite element models provide an accurate and reliable tool for structural design. However, they offer more of a physically justified reference than a precise answer when it comes to adjusting to actual measurements in operation. For any simulation, it is essential to properly idealize the structure and avoid modeling errors in order to obtain a reliable reference. In this work, two finite element models have been developed: (1) A shell-type model in SAP2000 that has 2D elements with associated sections (thicknesses) and produces reference results for natural frequencies, mode shapes, rotations and deflections;

(2) A solid model in ANSYS that has no associated sections because it is defined by 3D geometry and provides, among other results for comparison with the first model, strains and stresses on the faces.

Although they are not the same, in terms of finite element modeling, a Load Test would be comparable to permanent monitoring, since the dead weight, dead loads, and prestressing had already been transferred to the structure before the instrumentation was installed. Therefore, the sensor measurements will only include the part corresponding to live loads, and the principle of superposition hypothesis for linearly elastic structures is considered valid. The objective of this work is not to perform a thorough finite element model updating. However, both finite element models are approximately coincident, and the analytical natural frequencies are within the same range as those obtained from acceleration measurements on the bridge, within reasonable limits, after slightly adjusting upwards the overall elastic modulus of the models.



Figure 4: First three eigenmodes given by the SAP2000 shell model. The first mode is predomintaly lateral, and the second and third modes corresponds to vertical modes. The frequencies obtained (f1 = 3.29 Hz, f2 = 5.89 Hz, f3 = 6.33 Hz) are similar to those measured (f1 ≈ 3.3 Hz, f2 ≈ 5.4 Hz, f3 ≈ 6.5 Hz).

Furthermore, it can be observed that the global vibration modes capable of mobilizing practically the entire mass of the structure occur at frequencies between approximately 3 and 9 Hz, which would be within the range of action of the hydraulic hammer (incorporated into a railway excavator) used to modify the ballastless track superstructure prior to rail replacement operations. Although the railway renovation works are scheduled for completion in 2026, most of the concrete crushing had been accomplished by the end of June 2025, before the

permanent monitoring system was installed. However, TECSA, the construction company responsible for the works, carried out initial punctual measurements confirming that the accelerations generated by the hydraulic hammer were comparatively lower than those generated by passing trains. TECNALIA also made a subsequent visit, when the hammering work was halfway through, and measured the accelerations during a night's work at the end of May 2025. Using a USB-C MEMS sensor (PicoQuake from PLab) connected to a smartphone acting as a data logger thanks to Tecnalia's FuturAPP mobile app (TXu002451246), acceleration signals were recorded with similar conclusions. The first four natural frequencies were also identified thanks to the excitation produced by the aforementioned works.

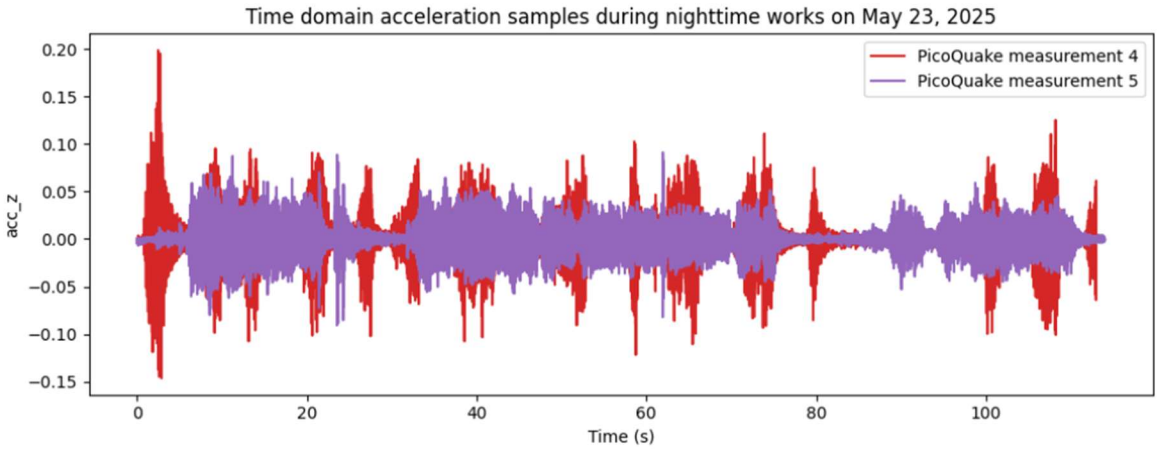


Figure 5: Sample of the two records with the highest vertical accelerations (in g) recorded with the MEMS sensor connected to a smartphone during the night works mentioned above. Once in place, the permanent monitoring system will control operational acceleration limits in real time against existing normative thresholds.

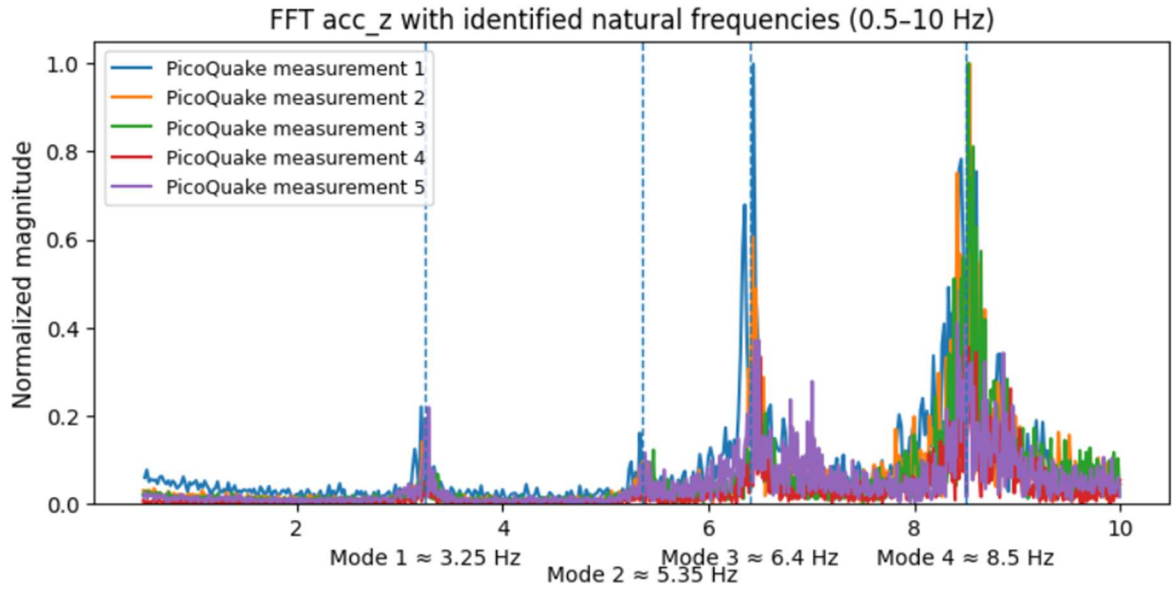


Figure 6: Natural frequencies identified from preliminary measurements taken with the MEMS sensor connected to a smartphone during concrete crushing works to modify the railway platform of the bridge.

Despite the inherent inaccuracy in identifying natural frequencies from vibration records generated on the bridge by the aforementioned machine and measured with the MEMS sensor, the values obtained are approximately equal to those identified from ambient vibrations

measured with force balance accelerometers after the installation of the permanent monitoring system. Therefore, based on the available data, the modifications made to the superstructure would not have had an appreciable effect on the stiffness and mass balance of the structure.

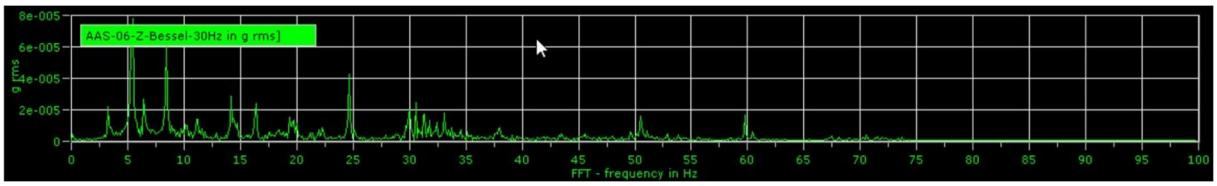


Figure 7: Detail of an FFT of environmental vibration collected by the continuous monitoring system, in which frequencies in the same range can be observed (f1 ≈ 3.3 Hz, f2 ≈ 5.4 Hz, f3 ≈ 6.5 Hz, f4 ≈ 8.5 Hz).

In summary, in terms of natural frequencies, the preliminary measured behavior, the behavior recorded by the permanent monitoring system, and the results of the finite element models are reasonably consistent. Similarly, after simulating a standard train with the calibrated models, analytical deflection values are close to those measured topographically in the 2003 opening Load Test. Thus, we can consider that the initial condition of the bridge is a good reference for establishing a continuous monitoring system such as the one described in this paper. Further comparisons cannot be made in this case, as neither deflections nor strains can be measured with sensors due to the inaccessibility of the underside of the bridge.

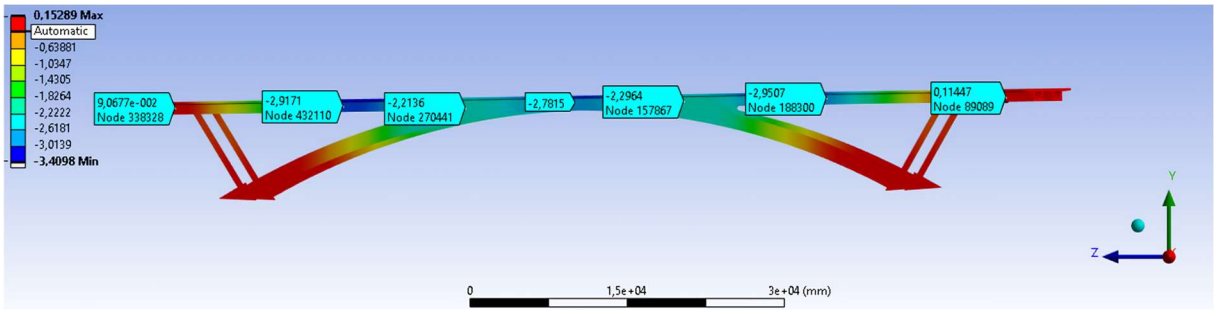


Figure 8: Deflections obtained by the ANSYS solid model after positioning a standard train on both tracks (load coefficients for a train full of passengers and dynamic factors extracted from the documentation by Carlos Fernández Casado S.L. for the 2003 opening Load Test).

2.3 Convolutional Neural Network

In this paper, the contribution in AI was made by training a CNN with 24 hours of acceleration data and implementing it online to obtain a real-time response. In this way, we initially limit the risk of overfitting and propose an application that is not entirely deterministic. In other words, the algorithm put into service is capable of classifying the vast majority of new cases as normal, but there will always be scenarios that have not been seen before. Therefore, we will focus on displaying whether the proportion of anomalies evolves rather than giving an absolute yes or no answer (this is explained visually with a heat map in the results section of this article).

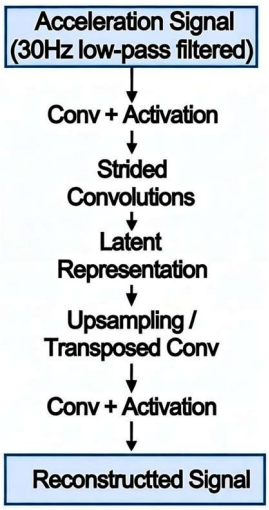


Figure 9: High-level flow of the implemented algorithm, which in particular responds to the architecture of a CNN autoencoder for numerical data, where reconstruction error is used as a metric for anomalies.

The accelerations, which are sent pre-filtered with a 30 Hz low-pass Bessel filter, are processed in windows so that each training record lasts 60 seconds, with records captured at a rate of one per minute. The algorithm must be pre-trained (with data collected by the online system) before being put into service. After observing its performance trained with 24 hours of data, it should be progressively trained with a larger amount of data. This will be part of the future work to be carried out within the framework of this case study. However, preliminary results of training with a larger amount of data will be analyzed in later sections.

Thanks to this AI algorithm, the online control panel will display an updated heat map with bands indicating levels of normality and colors quantifying the population or number of data classified in each band. In addition, health indicators will also be tracked to monitor the mean square error and the probability of normality, understood as the translation of the error into a confidence interval.

3 RESULTS

3.1 Automatic thresholds

Before being sent to the cloud, acceleration measurements are acquired at a sampling frequency of 200 Hz and then filtered through a 30 Hz Bessel low-pass filter. The monitoring architecture is prepared for the transmission and storage (both local and in the cloud) of the data generated due to the characteristics mentioned in a previous section. The assessment of the operational bridge safety of railway bridges is governed by Eurocode EN 1990 A2, which restricts the vertical acceleration of the deck. For ballastless railway bridges, this limit is 0.5 g. The origin of this value is unknown, but it is believed to be the result of applying an arbitrary safety factor of 2 to accelerations of approximately 1 g in order to maintain contact between the wheel and the rail [9]. This hypothesis is questioned in the aforementioned study and in other research, which also points out that the limit for ballastless tracks has not been established empirically or scientifically, unlike the limit for ballasted tracks. In any case, it is important to remember that the limits mentioned apply to accelerations with components up to 30 Hz. In general, the accelerations measured by the system are below the indicated limit of 0.5 g. Moreover, we are being conservative in this regard with the use of a Bessel-type filter, which is not a strict cutoff. However, the purpose of this monitoring work is not to address the condition of the track or the railway platform, but only the structure of the bridge.



Figure 10: Real-time control panel for the level of vertical bridge deck acceleration (Eurocode EN 1990 A2). The maximum accelerations are graphically represented for the appropriate time windows. If the threshold exceeds 0.5 g, an automatic alert is sent by email to the infrastructure administrator (METRO BILBAO) and the person responsible for track renovation works (TECSA). The control panels are available at all times to METRO BILBAO, TECSA, and TECNALIA through controlled IP access.

Complementary IoT accelerometers, which must be configured to measure at 60 Hz (with no filter) in order to minimize measurement interruptions, yield similar conclusions. Also, in terms of tilt measurement, it is noteworthy that the values recorded by the electrolytic transducer inclinometer are small, with variations around 0.15 degrees controlled by the passage of trains and the accuracy of the sensor itself.

3.2 CNN heat map and indicators

The pre-trained AI is capable of generating the following inferences, which are permanently available in real time:

- A probability heat map, which shows the CNN model's evaluations in an easily interpretable way. This graph represents the distribution of the probability that the bridge's behavior will be “normal” over time. The algorithm has been fed with time series (windowed data) of accelerations due to the train, free vibration, and environmental vibration recorded by force balance accelerometers (with high sensitivity, 5 V/g configured in a range of ±2 g). After training, the 95th percentile of reconstruction errors was set as the threshold for anomaly detection. As an intuitive and general view of the inference, the red bands on the heat map indicate a high density of cases, and the upper band indicates a high probability of “normal” behavior. In summary, if the bridge works as learned, this will mean that only the upper band would be red or orange and the rest, sparsely populated, green.



Figure 11: Detail of the heat map generated with CNN inferences. If the red band occupies lower positions over time, it could mean that: (i) the network needs to be retrained because there are many normal cases that the algorithm does not recognize, (ii) there is overfitting in the neural network, or (iii) the structure responds differently due to damage. Finding an optimal training strategy to minimize false positives due to (i) and (ii) will be a key aspect of future work.

- Control panel with real-time graphical representation of error metrics, allowing warnings to be sent. However, these must be interpreted using the heat map, which provides a broader context of the situation and allows the determination of whether the structure is behaving abnormally on a consistent basis.



Figure 12: Real-time graph of mean square error (green), threshold (orange) for sending warnings based on that value, and probability of normality (yellow). A value close to 1.0 for the latter indicator confirms that the structure is healthy according to the reference state (i.e., the measured state).

The results shown above are inferences made by the algorithm after being trained with 24 hours of data, resulting in a heat map that is surprisingly functional with only this information. Furthermore, although this aspect needs to be studied in greater depth, the CNN has also been trained with one month of continuous monitoring data (43,123 records of 60-second windows sampled every minute). The resulting heat map reveals improved performance compared to the 24-hour training heat map. The distribution is more concentrated in the upper normality bands (probability > 0.85), with a significant reduction in the population in the lower green bands, indicating that the model better recognizes normal operational patterns. This improvement suggests that increasing the training dataset reduces false positives without evidence of overfitting, as the vast majority of new cases continue to be correctly classified as normal.

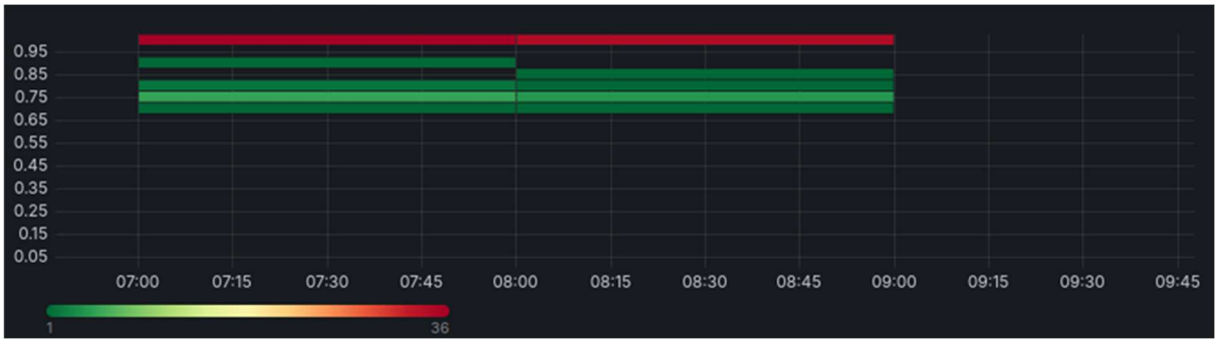


Figure 13: Heat map after training with one month of data (43,123 records), showing a more concentrated distribution in high-probability bands and fewer cases in lower probability zones compared to 24-hour training.

To further analyze the performance of the CNN with expanded training data, we proceed to study the distribution of reconstruction errors across the entire one-month training dataset. The resulting histogram reveals the model's ability to accurately reconstruct normal operational patterns, with the vast majority of samples concentrated around an error close to zero. The reconstruction error would follow the expected distribution for an autoencoder trained on healthy structural behavior, where most cases would be reconstructed with minimal error and only a small tail of samples would exhibit higher reconstruction errors.

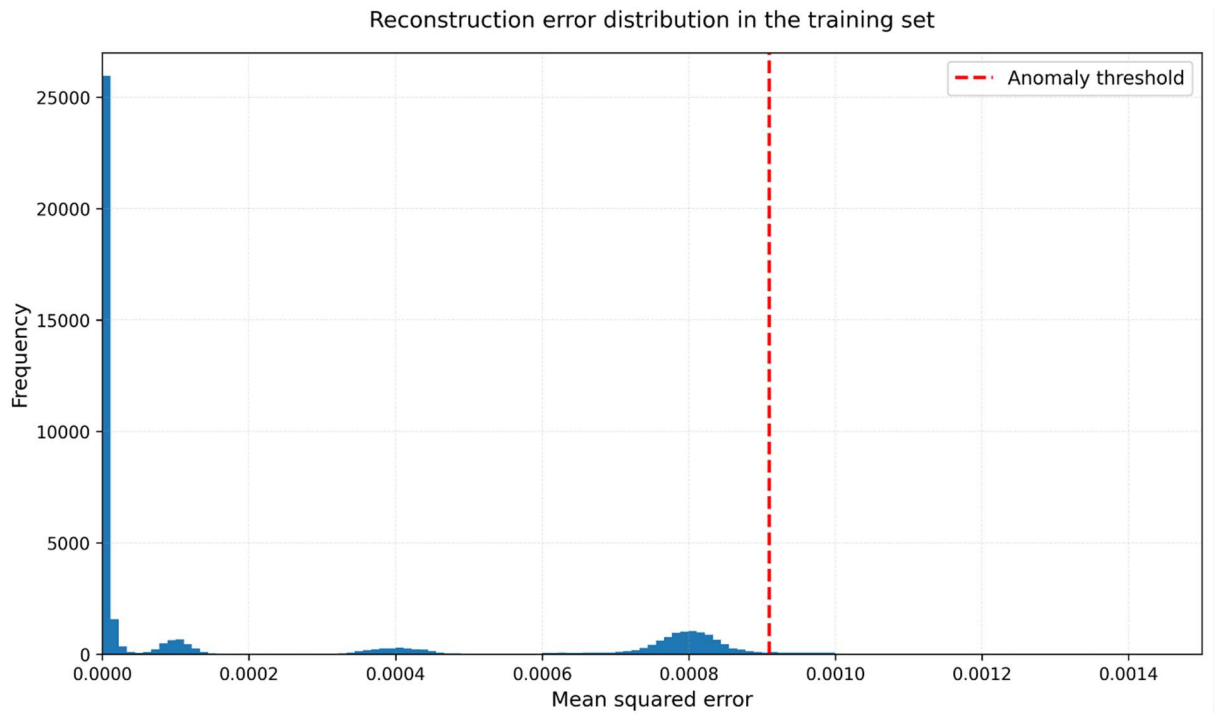


Figure 14: Distribution of reconstruction error in the training set (43,123 records). The anomaly threshold (red dashed line) was set at the 95th percentile of reconstruction errors, corresponding to a mean squared error of approximately 0.001.

The anomaly threshold, marked by the red dashed line, was established at the 95th percentile of the reconstruction error distribution. This statistical approach ensures that 95% of normal operational cases are correctly classified, while providing sufficient sensitivity to detect potential anomalies. Without prejudice to a more comprehensive long-term study, the clear separation between the main peak and the threshold indicates that the model has learned robust representations of the bridge's normal behavior without overfitting to specific operating

conditions. This threshold setting strategy would balance the trade-off between false positive rates and detection sensitivity, which is critical for practical implementation in real-time monitoring systems, where false alarms can undermine user confidence in the system.

4 CONCLUSIONS AND FUTURE WORK

- Based on the data considered in this paper, no damage to the bridge structure was identified after analyzing the available results and comparing them with the finite element models. It is essential to note that the analysis begins at the moment the measurements start. In other words, neither the original reference on the bridge's natural frequencies and accelerations nor information on any changes that may have occurred in the bridge since its construction is available.
- Once the permanent monitoring system was installed, automatic email notifications were set up to check whether normative bridge deck acceleration limits were exceeded (for accelerations with components up to 30 Hz). The accelerations caused by passing trains, although high, are clearly below the limit set for ballastless tracks. In addition, the acceleration generated by the works to replace the old rails with new ones is small. Regarding these works, the accelerations caused by the breakage of the concrete superstructure necessary for this replacement have not been measured by the permanent monitoring system. However, punctual measurements taken before the system was put into operation suggest that these accelerations are comparable to those generated by passing trains.
- The monitoring system is capable of processing data at high sampling rates, and the implemented CNN can provide intelligent diagnostics in real time. The heat map generated provides a visual assessment with sufficient flexibility to avoid false alarms about the observed behavior being normal according to the learned pattern. In this case, only the upper band of the heat map or the strip with a high normality index is red or orange (densely populated) and the lower bands are green (with few cases, as there will always be some patterns not seen). In the event of an alert, some lower bands of the heat map would no longer be green.
- Training the CNN with one month of operational data (43,123 records) significantly improved the algorithm's performance. The reconstruction error distribution shows a concentrated peak near zero with a clear anomaly threshold at the 95th percentile. The resulting heat map demonstrates better discrimination of normal behavior, with fewer false classifications in low-probability bands. This validates the scalability of the approach and suggests that continued training with additional operational data will further refine the model's sensitivity to actual anomalies while maintaining robustness against normal operational variability.
- Future studies will investigate optimal training strategies and the sensitivity of the anomaly ratio in inferences as an indicator of degradation progression. However, the prestressing condition of the bridge is unknown, as there is no initial reference and, in general, it has not been proven that inertial sensors can effectively detect prestressing problems when there are no external tendons available for direct measurement. However, treating bridge acceleration records as signatures allows subtle changes in signal patterns to be detected, so they could show greater sensitivity than vibration features (natural frequencies, mode shapes) to such problems. In other words, beyond the implicit vibration characteristics, there is explicit information on operational variability in the time-domain measurement of acceleration, which constitutes a local variable that provides a wealth of

information that can be characterized at more than one point (sensor) using artificial intelligence techniques. In any case, no monitoring system avoids testing when it is prescribed, and a principal inspection of the bridge, including its hard-to-reach areas, is recommended once the track renovation work is completed. This will also provide a better understanding of the baseline conditions for the purposes of continuous monitoring, which is recommended to be maintained in the long term, and, where appropriate, to supplement the current instrumentation with additional sensors.

5 ACKNOWLEDGMENTS

TECNALIA would like to thank METRO BILBAO and TECSA, respectively the infrastructure administrator and the company responsible for the Etxebarri arch bridge rail track renovation works. The authors would also like to express their gratitude to the Horizon Europe (HE) program within the FUTURAL project (GA 101083958), where they conduct research on AI applied to bridges, and the MULTICLIMACT project (GA 101123538), where they work on monitoring system architectures.

REFERENCES

[1] J. Brownjohn, A. De Stefano, Y. Xu, H. Wenzel and others, "Vibration-Based Monitoring of Civil Infrastructure: Challenges and Successes," Journal of Civil Structural Health Monitoring, vol. 1, no. 3-4, https://doi.org/10.1007/s13349-011-0009-5, 2011

[2] S. Saidin, A. Jamadin, S. Abdul Kudus and others, "An Overview: The Application of Vibration-Based Techniques in Bridge Structural Health Monitoring," International Journal of Concrete Structures and Materials, vol. 16, no. 69, https://doi.org/10.1186/s40069-022-00557-1, 2022

[3] F. Magalhães, À. Cunha and E. Caetano, "Dynamic Monitoring of a Long Span Arch Bridge," Engineering Structures, vol. 30, no. 11, https://doi.org/10.1016/j.engstruct.2008.04.020, 2008

[4] P. Anastasopoulos, K. Maes, G. De Roeck, G. Lombaert and E. Reynders, "Influence of Frost and Local Stiffness Variations on the Strain Mode Shapes of a Steel Arch Bridge," Engineering Structures, vol. 273, no. 115097, https://doi.org/10.1016/j.engstruct.2022.115097, 2022

[5] A. Fernandez-Navamuel, D. Pardo, F. Magalhaes, D. Zamora-Sanchez and others, "Deep Neural Network for Damage Detection in Infante Dom Henrique Bridge using Multi-Sensor Data," Structural Health Monitoring, vol. 24, no. 1, https://doi.org/10.1177/14759217241227455, 2024

[6] J. Lee, H. Kim, S. Kim and H. Lee, "Evaluation of Structural Integrity of Railway Bridge using Acceleration Data and Semi-Supervised Learning Approach," Engineering Structures, vol. 239, no. 112330, https://doi.org/10.1016/j.engstruct.2021.112330, 2021

[7] O. Avci, O. Abdeljaber, S. Kiranyaz, M. Hussein and D. Inman, "Wireless and Real-Time Structural Damage Detection: A Novel Decentralized Method for Wireless Sensor Networks," Journal of Sound and Vibration, vol. 424, no. https://doi.org/10.1016/j.jsv.2018.03.008, 2018

[8] A. Armijo and D. Zamora-Sanchez, "Integration of Railway Bridge Structural Health Monitoring into the Internet of Things with a Digital Twin: A Case Study," Sensors, vol. 24, no. 7, https://doi.org/10.3390/s24072115, 2024

[9] G. Ferreira, P. Montenegro, A. Andersson, A. Henriques, R. Karoumi and R. Calçada, "Critical Analysis of the Current Eurocode Deck Acceleration Limit for Evaluating Running Safety in Ballastless Railway Bridges," Engineering Structures, vol. 312, no. 118127, https://doi.org/10.1016/j.engstruct.2024.118127, 2024